

# Effects of the Cure Cycle and Thermoplastic Content on the Final Properties of Dicyanate Ester/Polysulfone Semi-IPNS

I. HARISMENDY,<sup>1</sup> M. DEL RIO,<sup>1</sup> A. VALEA,<sup>1</sup> JNA. GAVALDA,<sup>2</sup> I. MONDRAGON<sup>1</sup>

<sup>1</sup> Dpto. Ing. Química y M. Ambiente, Escuela Ingeniería T. Industrial, Universidad del País Vasco/Euskal Herriko Unibertsitatea, Avd. Felipe IV, 1 B. 20011 San Sebastián/Donostia, Spain

<sup>2</sup> Departament de Química Física e Inorgánica, Universitat Rovira y Virgili, Plaça Imperial Tàrraco, 1. 43005 Tarragona, Spain

Received 19 July 2000; accepted 10 May 2001

**ABSTRACT:** A bisphenol A dicyanate resin, BADCy, was toughened by incorporating polysulfone, PSU, at various compositions. The catalyst system used was a mixture of copper acetylacetonate and nonylphenol. Phase separation and rheokinetics were studied through curing. The blends seemed to have a LCST behavior, and the presence of PSU did not affect the polycyclotrimerization kinetics. The phase structure, thermal, and mechanical properties of the final network were investigated as a function of the PSU content and cure temperature. The toughness of the BADCy/PSU blends was closely related to their final morphology, increasing with the amount of phase inversion. The mechanical properties were not affected by the addition of the thermoplastic. © 2002 John Wiley & Sons, Inc. *J Appl Polym Sci* 83: 1799–1809, 2002

**Key words:** phase separation; morphology; toughness

## INTRODUCTION

The increasing demands of the aerospace and electronic industries for new high-performance structural applications with a combination of thermal, mechanical, and electrical properties have motivated the development of new thermosetting resins like the cyanate esters. Commercial uses for these resins include applications such as multilayer circuit boards, electronic encapsulants, microwave antennas, and aircraft and aerospace components. They have excellent properties like low dielectric losses, low moisture absorption, good adhesive properties, and glass transition

temperatures in the range of 250 to 300°C.<sup>1–3</sup> Although cyanates are known to be relatively tough compared with other thermosetting matrices,<sup>3</sup> some applications require improved fracture resistance.

Fracture toughness of these matrices can be improved by rubber incorporation but at the expense of high temperature performance.<sup>4</sup> The use of high-performance thermoplastics has the additional advantage compared to rubber modification that there is no reduction in thermal and mechanical properties of the cyanate matrix.<sup>5–7</sup>

The enhancement of the fracture toughness is closely related to the generated morphology, which is controlled by the content of thermoplastic, curing conditions, and materials used.<sup>8–10</sup> Because the morphology of the blends depends on two competing factors, phase separation, and matrix polymerization,<sup>8</sup> the various factors that influence the thermodynamics and kinetics of both

Correspondence to: I. Mondragon.

Contract grant sponsor: Dirección General de Ciencia y Tecnología (DGICYT); contract grant number: MAT95-0701.

*Journal of Applied Polymer Science*, Vol. 83, 1799–1809 (2002)  
© 2002 John Wiley & Sons, Inc.  
DOI 10.1002/app.10119

processes need to be studied to achieve an optimum morphology.

In this study, semi-interpenetrating polymer networks (Semi-IPNs) have been synthesized based on a high-temperature thermosetting dicyanate ester and a thermoplastic, polysulfone (PSU). To use industrial cure schedules, samples were catalyzed with a blend of nonylphenol and copper (II) acetylacetonate. The aim of this work was to study the effects of cure temperature and PSU content on the chemorheology of curing as well as on the morphology and on the related final properties of the mixtures.

## MATERIALS AND METHODS

The dicyanate ester used in this study was a bisphenol A dicyanate (BADCy) with the trade name AroCy B10 from Ciba, 99.5% purity, and with a cyanate equivalent of 139 g/Eq. The selected thermoplastic was a commercial grade polysulfone, PSU (Udel P1700), from Amoco. The catalyst system used was a mixture of 1.78 wt % of copper (II) acetylacetonate,  $\text{Cu}(\text{AcAc})_2$ , in nonylphenol, NP, both from Aldrich.

Modified cyanate resins containing 0–20 wt % PSU were prepared in the same way that was previously shown for BADCy/PEI mixtures.<sup>5</sup> Thermal, rheological, and cloud point measurements were carried out following the procedure previously published.<sup>5</sup> Microstructural studies were performed by dynamic-mechanical analysis, DMA, and scanning electron microscopy, SEM, by using the same sample preparation and tests conditions used for the BADCy modified with polyetherimide.<sup>5</sup>

For fracture testing, single-edge notched specimens ( $60 \times 12 \times 5 \text{ mm}^3$ ), SEN, were employed. A “V” notch was cut in the sample with a rotating cutter, and a starter crack was initiated with a razor blade. Test were performed in a three-point bending mode, following the ASTM-E399 standard specification with an Instron Universal Testing Machine, model 4206. Each reported value is the average of at least five measurements.

Flexural properties were determined in a three-point bending mode following the ASTM-D790 standard specifications in the same Instron machine at a crosshead of  $1.7 \text{ mm} \cdot \text{min}^{-1}$  using  $80 \times 10 \times 5 \text{ mm}^3$  specimens. At least five specimens were tested for every data point.

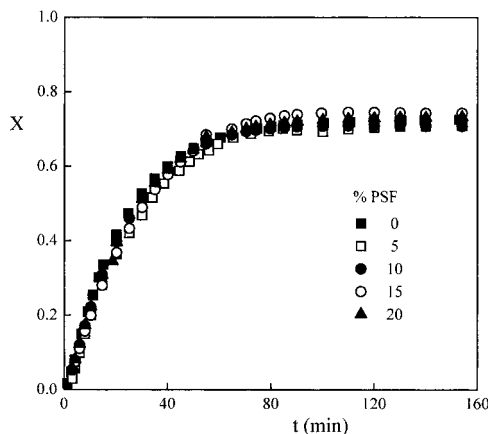


**Figure 1** Cyanate conversion profiles for BADCy based mixtures with 0–20 wt % PSU content cured at 150°C.

## RESULTS AND DISCUSSION

### Rheo-kinetics of Curing

Isothermal curing was carried out from 130 to 180°C each 10°C. All the samples were then subjected to a dynamic DSC scan at  $10^\circ\text{C} \cdot \text{min}^{-1}$  to determine the residual heat of reaction,  $\Delta H_{\text{res}}$ .

The conversion of each sample under isothermal conditions was calculated by:

$$X = \frac{(\Delta H_{\text{iso}})_t}{\Delta H_{\text{iso}} + \Delta H_{\text{res}}}$$

where  $(\Delta H_{\text{iso}})_t$  is the heat of reaction at a time  $t$  calculated from the isothermal mode, and  $(\Delta H_{\text{iso}} + \Delta H_{\text{res}})$  is the total heat of reaction obtained from the addition of the total heat from the isothermal mode,  $\Delta H_{\text{iso}}$ , and the residual one,  $\Delta H_{\text{res}}$ . Figure 1 shows the conversion profiles during curing at 150°C for the resin modified with several amounts of PSU. No significant influence on cure kinetics was observed. It has been reported that this commercial PSU is randomly terminated with chloro and phenol groups<sup>11</sup> or methoxy end capped groups.<sup>12</sup> Hwang et al.<sup>13</sup> studied the kinetics of noncatalyzed BADCy/PSU (Udel P-3500) mixtures. They observed that the Udel P-3500 acts as a catalyst for curing BADCy resins. This behavior was attributed to the presence of phenolic compounds included in the commercial PSU. In the case of the catalyzed resin, no significant changes kinetics are expected to take place with this kind of compounds.<sup>14</sup>

**Table I Gel Times and Conversions of the BADCy/PSU Mixtures at Different Precure Temperatures and PSU Contents**

PSU (wt %)	0		5		10		15		20	
	$t_{\text{gel}}$ (min)	$X_{\text{gel}}$	$t_{\text{gel}}$ (min)	$X_{\text{gel}}$	$t_{\text{gel}}$ (min)	$X_{\text{gel}}$	$t_{\text{gel}}$ (min)	$X_{\text{gel}}$	$t_{\text{gel}}$ (min)	$X_{\text{gel}}$
130	124	0.60	124	0.60	125	0.60	125	0.60	125	0.60
140	60	0.61	61	0.61	59	0.60	61	0.61	61	0.61
150	36	0.59	36	0.59	37	0.60	36	0.59	36	0.59
160	24	0.60	23	0.60	24	0.60	24	0.60	24	0.60
170	15	0.58	15	0.58	16	0.59	17	0.60	16	0.59
180	8	0.57	8	0.57	9	0.59	9	0.59	9	0.59

To confirm this behavior, rheological measurements were also performed. The gelation time was calculated as the time where the loss factor,  $\tan \delta$ , became independent of frequency using multiwave time tests.<sup>15</sup> The presence of PSU did not affect the gelation times or conversions, as it can be seen in Table I. The conversion at gelation times was between 0.57 and 0.61, similar to that found in the literature survey.<sup>16,17</sup>

#### Phase Separation Behavior

The uncured samples with 0–20% PSU content were transparent and homogeneous under the optical microscope at room temperature. Although the temperature was risen up to 100°C, no signs of phase separation were observed. Heating up to higher temperature was not possible due to the polymerization of the BADCy. To increase the temperature where the reaction starts, uncatalyzed mixtures were prepared. In this case, the temperature can be risen up to 200°C. Again, there was no phase separation, so the cloud-point curve (CPC) for the unreacted system could not be

obtained. The differences between the solubility parameters of the components are small,  $9.4 \text{ (cal} \cdot \text{cm}^{-3})^{1/2}$  for the BADCy and  $10.2 \text{ (cal} \cdot \text{cm}^{-3})^{1/2}$  for the PSU.<sup>18</sup> Taking this into account and the fact that a LCST, lower critical solution temperature behavior has been reported in the case of epoxy/PSU blends<sup>19,20</sup> one should expect a LCST behavior of the BADCy/PSU blends. The calculation of the theoretical critical concentration without considering the PSU polydispersity<sup>21</sup> gives a minimum at 7 wt % PSU content.

Table II shows the cloud-point times and conversions for the blends cured at several temperatures with 10, 15, and 20 wt % PSU. The mixtures with 5 wt % PSU did not show signs of phase separation. The fact that the lower cloud-point conversions were observed at higher cure temperatures and PSU contents confirmed the LCST behavior of the system. In the study of Hwang et al.<sup>13</sup> of the uncatalyzed BADCy/PSU (Udel P-3500) mixtures at temperatures ranging from 200 to 250°C, the phase separation conversions obtained were higher, and there was an increase

**Table II Cloud Point Times and Conversions for the BADCy/PSU Mixtures at Different Precure Temperatures and PSU Contents**

PSU (wt %)	10		15		20	
	$t_{\text{cp}}$ (min)	$X_{\text{cp}}$	$t_{\text{cp}}$ (min)	$X_{\text{cp}}$	$t_{\text{cp}}$ (min)	$X_{\text{cp}}$
130	79	0.47	65	0.42	67	0.43
140	42	0.48	39	0.47	38	0.47
150	24.5	0.45	18	0.38	18.5	0.38
160	13.5	0.41	12	0.39	11	0.37
170	7	0.38	6	0.32	5.5	0.29
180	5	0.40	4	0.32	3	0.27

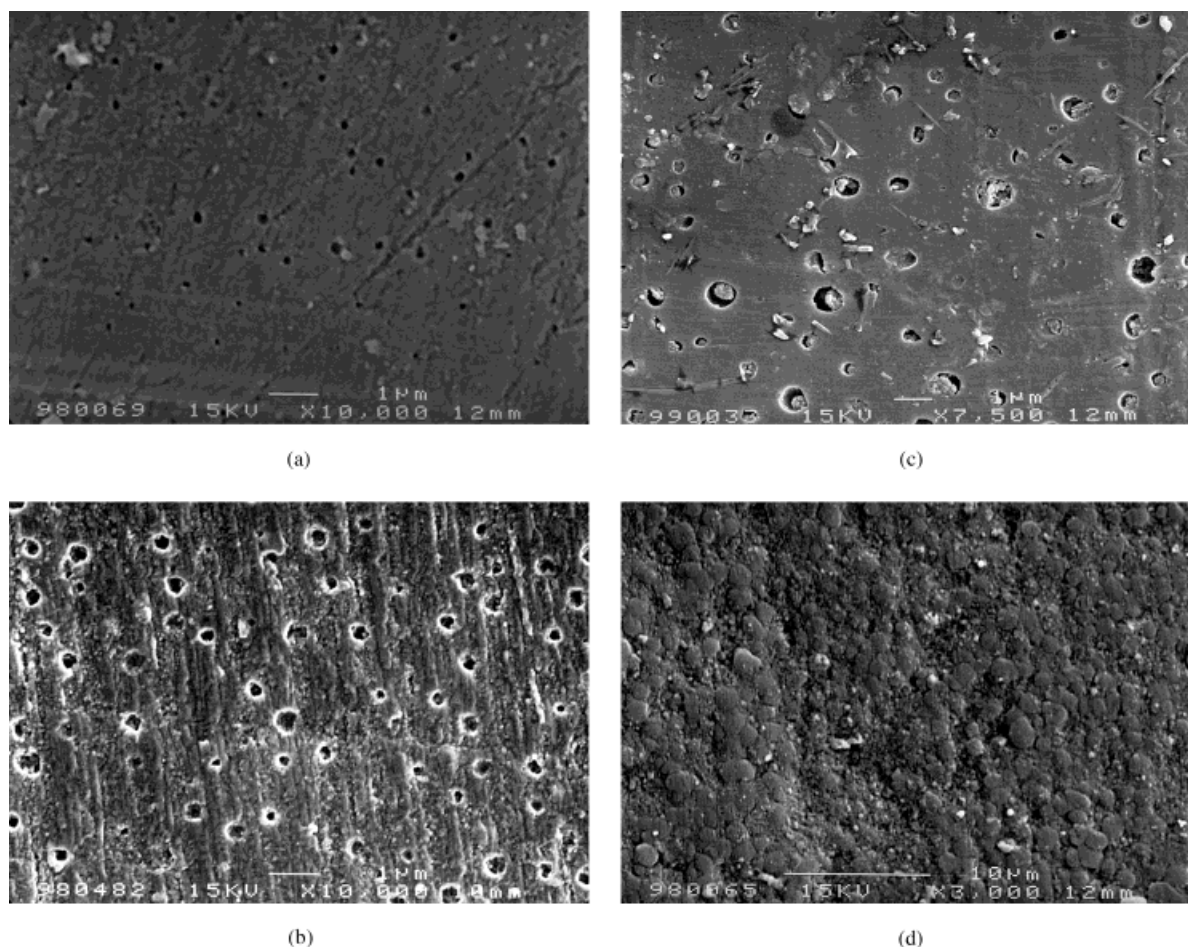


**Figure 2** Morphologies of the BADCy/PSU mixtures precured at 160°C etched with  $\text{CH}_2\text{Cl}_2$ : (a) 5 wt %, (b) 10 wt % PSU; and  $\text{H}_2\text{SO}_4$ : (c) 15 wt %, and (d) 20 wt % PSU.

in the cloud-point conversions with the cure temperature. This confirms the fact that factors like the cure temperature,  $T_c$ , kinetics (presence or absence of a catalyst), and modifier molecular weight play an important role in the phase separation behavior and resulting morphologies of these mixtures. Most of the morphological characteristics depend on the location of the critical conversion at the cloud point,  $X_{cp}$ , at which phase separation begins to take place with respect to the gel point,  $X_{gel}$ . If the conversion is very low compared to  $X_{gel}$  the system has a higher mobility when it reaches the cloud point and leads to a greater extent of demixing before the increasing viscosity of the blend halts the evolution of the phases.<sup>22</sup>

#### Microstructural Analysis

Figures 2(a)–(d) present the morphologies of the BADCy/PSU mixtures precured at 160°C. SEM

scans showed the presence of two distinct phases for every PSU contents and cure conditions used. Even for the 5 wt % PSU mixture [Fig. 2(a)], a high magnification ( $\times 10,000$ ) reveals that there are some scattered particles of submicrometre size (0.05–0.15  $\mu\text{m}$ ) of PSU dispersed in the BADCy-rich matrix. In this case, phase separation was not detected by optical microscopy because this technique is not sensitive to the presence of dispersed particles with that size.<sup>23</sup>

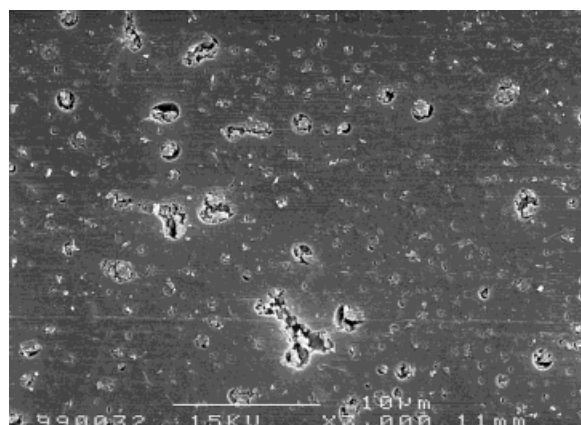
When the PSU content was increased to 10 wt % [Fig. 2(b)] the size of the microspheres increased up to 0.2–0.4  $\mu\text{m}$ , and phase separation could be detected by optical microscopy. The particle size distribution is not uniform, at least two particle sizes are observed. This kind of distribution is usually preferred to the unimodal distribution because it produces a higher increase in the fracture toughness.<sup>24</sup> Hwang et al.<sup>25</sup> reported



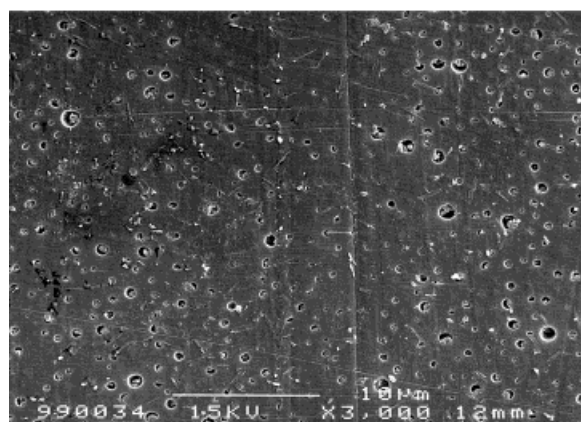
a similar morphology for the uncatalyzed BADCy resin modified with 10 wt % of PSU Udel P-3500. However, the particle size was higher (0.5–1  $\mu\text{m}$ ) probably because of the different phase separation behavior of the mixtures previously commented. Although not shown, similar morphologies were found at 140 and 180°C precure temperatures.

At 15 wt % PSU contents [Fig. 2(c)] a complex morphology was observed: there seems to be small particles of BADCy dispersed in the PSU-rich dispersed domains. This dual phase morphology is believed to be formed by an evolution of a secondary phase in the already phase-separated domains due to abrupt changes of equilibrium composition and viscosity during cure.<sup>26</sup> This composition would be close to the critical point at which phase inversion occurs.

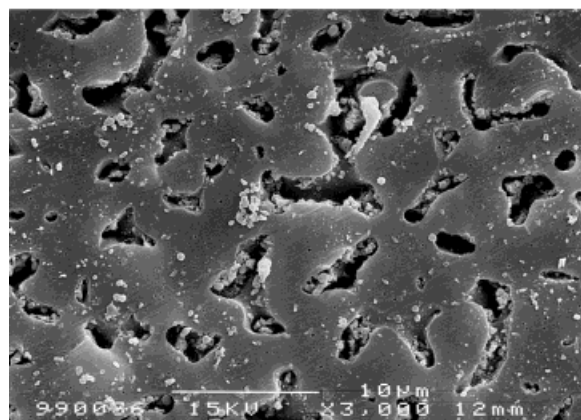
Although the calculated critical concentration for the uncured mixture was 7 wt % PSU, this critical point moves to higher thermoplastic concentrations as cure reaction progresses.<sup>8</sup> As it can be seen in Figure 3(a)–(c), the generated morphologies at this composition were highly influenced by the precure temperature. At 140°C there are small spherical domains and some bigger PSU domains of irregular shape. At 160°C PSU spherical domains mainly form the structure. At 180°C big PSU domains of irregular shape typical of a spinodal decomposition<sup>8</sup> form the structure. To confirm that behavior, unetched fracture surfaces were also observed. Figure 4(a)–(c) shows the fracture surfaces of the 15 wt % PSU precured at the three temperatures. The observed structures were similar than that for the unbroken etched samples. The presence of a secondary phase separation with BADCy particles in the PSU-rich phase is clearly evident in the micrographies. The roughness of the fracture surface is increased with increasing the PSU domains. The differences observed in the above shown micrographies could be related to the different mechanisms involved in the phase-separation process, depending on the cure temperature. Yoon et al.<sup>20</sup> studied the LCST phase behavior of an epoxy/PSU blend. They gave experimental evidence by using optical microscopy that the dual phase morphology was formed by a nucleation and growth (NG) mechanism followed by a spinodal decomposition (SD) one due to an abrupt change in viscosity. The mechanism of phase separation depends on two competing factors—phase separation, and polymerization rates. Usually, high temperatures favor SD decomposition.<sup>26</sup> So, the 140°C precured mixture



(a)



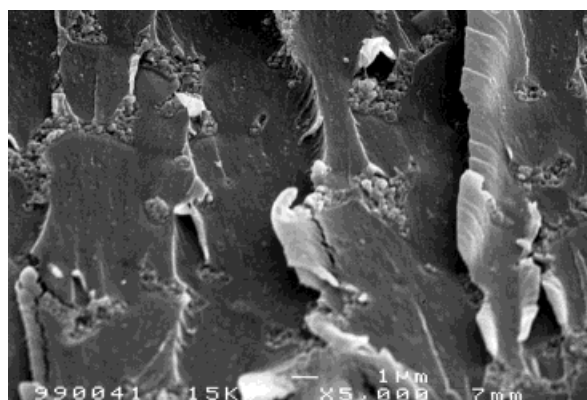
(b)



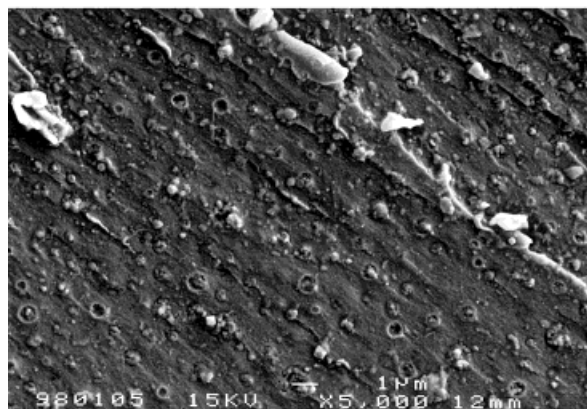
(c)

**Figure 3** Morphologies of the  $\text{H}_2\text{SO}_4$  etched 15 wt % PSU containing mixtures precured at (a) 140°C, (b) 160°C, and (c) 180°C.

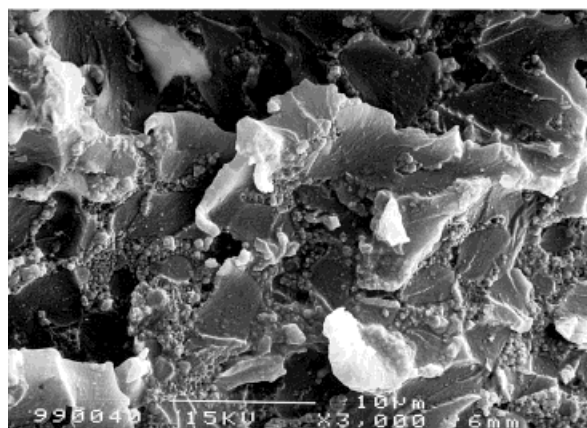
could have started the phase separation in the metastable region, between the spinodal and the binodal curves, with a NG mechanism. Then, it



(a)



(b)



(c)

**Figure 4** Unetched fracture surfaces of the 15 wt % PSU containing mixtures precured at (a) 140°C, (b) 160°C, and (c) 180°C.

could have fallen in the unstable region with a secondary phase separation via SD. The 160°C precured blend could have had a more complete phase separation in the metastable region due to

the lower viscosity of the medium. The system could have reached the unstable region at the time of structural freeze-in by gelation, with the spinodal decomposition only producing a BADCy precipitation in the already fixed PSU particles. In the 180°C precured blend it seems that the rate of phase separation was so high (the NG process is recognized to be slow<sup>8</sup>) that the system could have passed quickly the NG region and proceeded only to the SD mode. Work is in progress to elucidate the exact mechanism of phase separation in these mixtures.

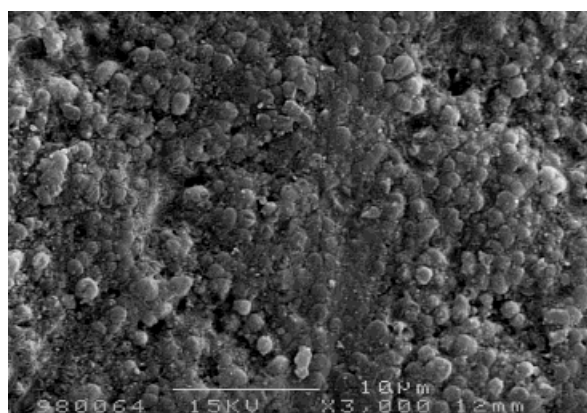
At 20 wt % PSU contents the blends showed complete phase inversion at the three cure temperatures. As it can be seen in Figure 2(d), the PSU phase formed the matrix and the BADCy appeared as big, interconnected, spherical domains of around 1–2  $\mu\text{m}$ . This morphology is generally attributed to a SD mechanism.<sup>5</sup> Again, the size of the particles was smaller than that found by Hwang (4–8  $\mu\text{m}$ ) with the Udel P-3500.<sup>25</sup> As shown in Figure 5(a)–(b), the size of the particles slightly increased for the 180°C cure temperature, probably due to the lower viscosity of the PSU forming phase during curing, which made BADCy particles grow more easily.

#### Dynamic Mechanical Analysis

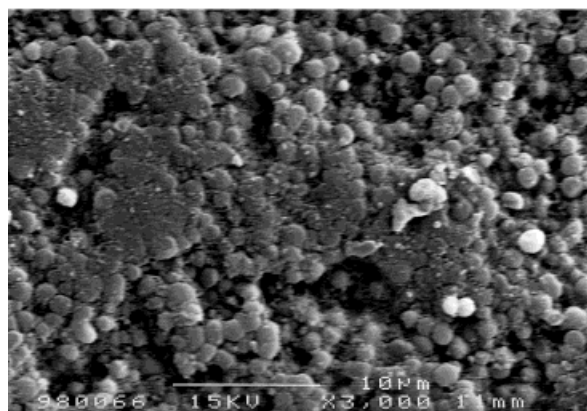
Mixtures were also examined using DMA at 10 Hz as this technique can give more information on microstructure of cured mixtures providing details about molecular mixing and phase continuity. Figure 6(a)–(b) shows the storage modulus and loss factor variations with temperature for the BADCy/PSU blends precured at 160°C. The viscoelastic spectra exhibited two  $E''$  relaxation peaks due to both separated phases, which approximately corresponded to those of the pure components. The relative evolution of these relaxations confirmed the above-shown phase inversion phenomena. As the PSU concentration was increased, the magnitude of the  $\alpha$  relaxation of the PSU-rich phase with respect to that for the BADCy-rich phase increased. For compositions equal or lower than 15 wt % PSU, the peak area of the BADCy-rich phase was larger than those of the PSU-rich phase, indicating that the BADCy formed the matrix in that composition range. For the 20 wt % PSU-containing mixture, the magnitude of the relaxation corresponding to the PSU-rich phase was much larger than that for the BADCy-rich phase, showing that phase inversion had occur, so becoming the PSU-rich phase the



matrix. These results are in agreement with the morphologies above reported by SEM. Figure 7 shows the loss modulus of the 15 wt % PSU-containing mixtures precured at different temperatures. The results confirm the morphologies observed by SEM. At 140°C the relaxation of the PSU-rich phase is bigger to that precured at 160°C, meaning that there is more PSU that has phase separated. At 180°C the  $T_g$  relaxation of the PSU-rich phase sharply increases, showing a typical dual-phase morphology shape. The relaxations of the PSU-rich and the BADCy-rich phases moved closer to each other. Table III shows the  $T_g$ s of the BADCy-rich phase,  $T_{g\alpha}$ , and the PSF-rich one,  $T_{g\beta}$ , in the mixtures taken as the maximum in the loss factor curves. The changes in both  $T_g$ s at the higher precure temperature could be attributed to a change in the concentration of PSU and cyanate in the phase-



(a)



(b)

**Figure 5** Morphologies of the  $H_2SO_4$  etched 20 wt % PSU containing mixtures precured at (a) 140°C and (b) 180°C.

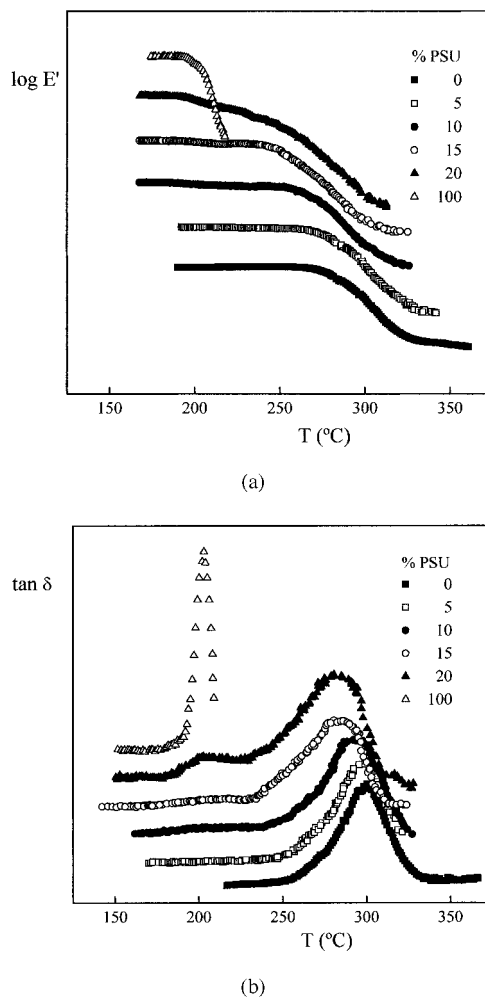


**Figure 6** (a) Storage modulus variation with temperature for the BADCy/PSU mixtures precured at 160°C. (b) Loss factor variation with temperature for the BADCy/PSU mixtures precured at 160°C.

separated regions. The Fox equation, widely used for miscible mixtures,<sup>27</sup> was used to calculate the composition of each phase:

$$\frac{1}{Tg_{\alpha}} = \frac{\varphi^{\alpha_1}}{Tg_1} + \frac{\varphi^{\alpha_2}}{Tg_2} \quad \text{and} \quad \frac{1}{Tg_{\beta}} = \frac{\varphi^{\beta_1}}{Tg_1} + \frac{\varphi^{\beta_2}}{Tg_2}$$

where the superscripts  $\alpha$  and  $\beta$  represent the cyanate and PSU-rich phases, respectively,  $\varphi$  has been taken as the weight fraction, and the 1 and 2 subscripts correspond to cyanate and PSU. Although it is only an approximation, these equations can give an idea of the amount of PSU and cyanate dissolved in the cyanate and PSU-rich phases. As can be seen in Table IV, there is an increase of the second component dissolved in

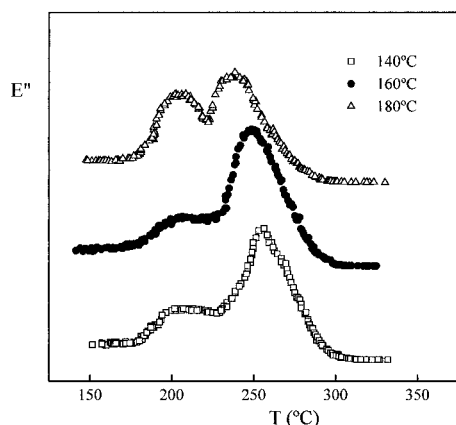


**Figure 7** Loss modulus of the 15 wt % PSU containing mixtures precured at different temperatures.

each phase with the cure temperature. This could support the fact that phase separation occurred via a spinodal decomposition for the 15 wt % PSU composition. In the NG mechanism particles with an equilibrium composition appear and then grow up. In the spinodal mechanism, the composition of the separated phases changes continuously during phase separation,<sup>8</sup> so when phase separation stops, each phase has the  $T_g$  corresponding to the composition at that moment. On the other hand, the spinodal mechanism even could happen for the mixture with a 10 wt % PSU due to the fact that the  $T_g$  of the BADCy for the sample cured at 180°C appeared at slightly lower temperatures than those for the mixtures precured at 140 and 160°C.

No significant variations were found in the viscoelastic spectra for the mixtures with 20 wt % PSU contents precured at different temperatures. The temperature corresponding to the maximum of the  $\alpha$  relaxation of the PSU-rich phase,  $T_{g\beta}$ , was at the same temperature range than that for

the neat PSU, meaning that phase separation was complete, and there was no cyanate dissolved in this phase. However, some PSU remained in the cyanate phase, and the  $T_g$  decreased with respect to that for the neat cyanate matrix.

### Fracture Toughness

Figure 8(a)–(b) shows the stress intensity factor,  $K_{IC}$ , and the fracture energy,  $G_{IC}$ , of the BADCy/PSU mixtures precured at different temperatures as a function of the PSU content. The solid line indicates the  $K_{IC}$  calculated according to the rule of the mixtures:

$$K_{IC} = \phi_{\text{BADCy}} \cdot K_{IC\text{BADCy}} + \phi_{\text{PSU}} \cdot K_{IC\text{PSU}}$$

where  $\phi_{\text{BADCy}}$  and  $\phi_{\text{PSU}}$  represent the volume fractions of BADCy and PSU, respectively. The  $K_{IC}$  of the PSF,  $K_{IC\text{PSU}}$  was taken as  $3 \text{ MPa} \cdot \text{m}^{1/2}$ .

$K_{IC}$  was higher than the predicted by the rule of the mixtures for every PSU contents and cure conditions used. The 15 wt % PSU mixture did not show a toughness improvement with respect to the 10 wt % PSU one, except for the 180°C precured mixture. Although the effect of the temperature was masked between the experimental error, there seems to be an increase in the toughness of the 15 wt % PSU mixture with increasing the cure temperature, with both  $K_{IC}$  and  $G_{IC}$  increasing. The higher amount of phase inversion observed by SEM seems to enhance the fracture toughness of his mixture. In the case of the 20 wt % PSU blends, where complete phase inversion had occur, there was a higher increase in the fracture toughness. The increase on fracture toughness in the case of phase inverted morphologies is usually associated to the ductile deforma-

**Table III**  $T_g$  of the BADCy and PSU-Rich Phases at Different Precure Temperatures and PSU Contents

$T_c$ (°C)	140		160		180	
	$T_{g\alpha}$ (°C)	$T_{g\beta}$ (°C)	$T_{g\alpha}$ (°C)	$T_{g\beta}$ (°C)	$T_{g\alpha}$ (°C)	$T_{g\beta}$ (°C)
0	299	—	299	—	299	—
5	296	—	296	—	295	—
10	294	204	293	205	287	207
15	286	208	284	209	280	210
20	281	201	282	202	281	202
100	—	202	—	202	—	202



**Table IV** BADCy and PSU-Rich Phases Compositions at Different Precure Temperatures and PSU Contents

$T_c$ (°C)	140				160				180			
	$\alpha$		$\beta$		$\alpha$		$\beta$		$\alpha$		$\beta$	
Phase	$\varphi_{\alpha_1}$ (wt %)	$\varphi_{\alpha_2}$ (wt %)	$\varphi_{\beta_1}$ (wt %)	$\varphi_{\beta_2}$ (wt %)	$\varphi_{\alpha_1}$ (wt %)	$\varphi_{\alpha_2}$ (wt %)	$\varphi_{\beta_1}$ (wt %)	$\varphi_{\beta_2}$ (wt %)	$\varphi_{\alpha_1}$ (wt %)	$\varphi_{\alpha_2}$ (wt %)	$\varphi_{\beta_1}$ (wt %)	$\varphi_{\beta_2}$ (wt %)
0	100	0	—	—	100	0	—	—	100	0	—	—
5	98	2	—	—	98	2	—	—	97	3	—	—
10	96.5	3.5	3	97	96	4	4.5	95.5	91	9	7.5	92.5
15	90.5	9.5	9	90	89	11	10	90	86	14	12	88
20	87	13	0	100	87.5	12.5	0	100	87	13	0	100
100	—	—	0	100	—	—	0	100	—	—	0	100

tion of the thermoplastic matrix.<sup>28,29</sup> There seems to be slight increase of the toughness with the cure temperature, probably due to the slightly higher particle size observed by SEM. The  $K_{IC}$  and  $G_{IC}$  calculated values at 20 wt % PSU are higher than the reported by Hwang<sup>25</sup> with uncatalyzed BADCy/PSU Udel P3500 and in the same range than those reported by Woo<sup>28</sup> for BADCy/PSU Udel P1700 and Shimp<sup>30</sup> for the BADCy/PSU Udel P1700.

### Mechanical Properties

Figure 9(a)–(c) shows the flexural modulus, strength, and strain to break of the BADCy/PSU mixtures precured at 140, 160, and 180°C as a function of the PSU content. As can be seen in Figure 9(a), there were not significant changes in the flexural modulus of the BADCy when PSU was added. There was not also a significant increase in the flexural strength [Fig. 9(b)], taken into account the experimental error. So the modification with PSU has the additional advantage that the mechanical properties of the resin are maintained. The slight increase of the strain to fracture observed for the 20 wt % PSU [Fig. 9(c)] mixture agrees with the higher toughness shown above for this mixture.

### CONCLUSIONS

A high-temperature thermosetting bisphenol A dicyanate was modified with polysulfone at various compositions, ranging from 0–20 wt %. The

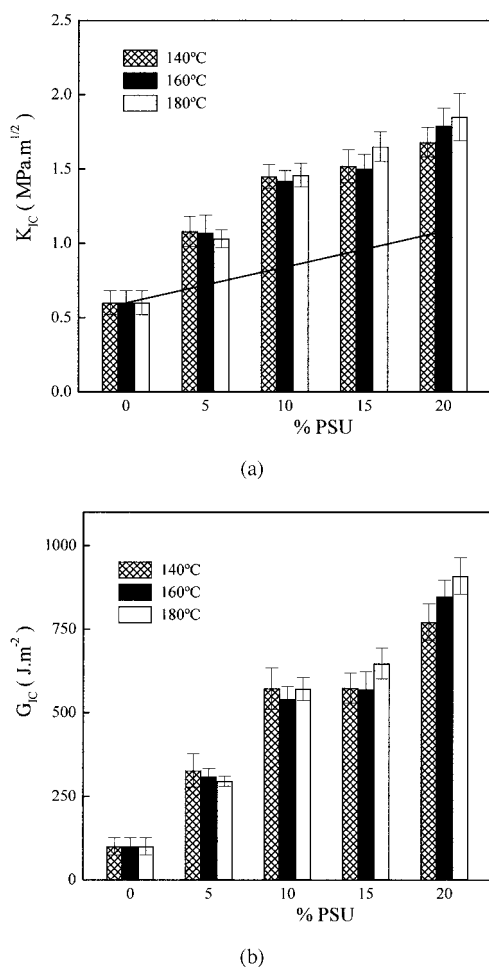


**Figure 8** (a) Stress intensity factor of the BADCy/PSU mixtures precured at different temperatures. (b) Fracture energy of the BADCy/PSU mixtures precured at different temperatures.

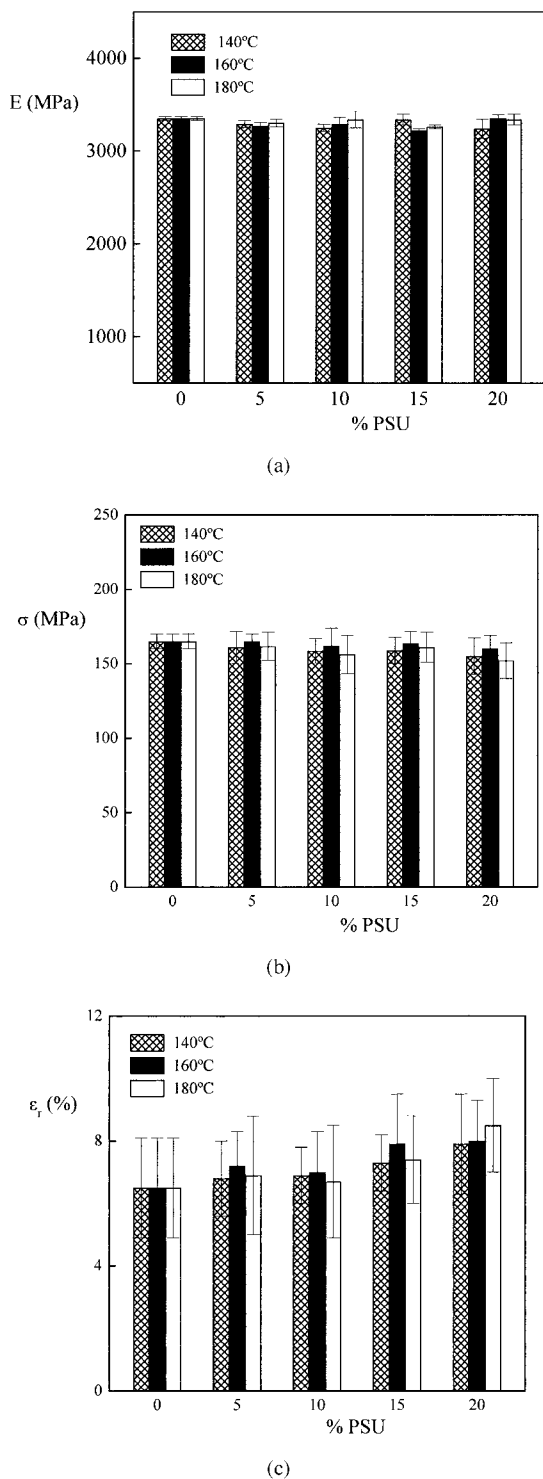


**Figure 9** (a) Flexural modulus of the BADCy/PSU mixtures precured at different temperatures. (b) Flexural yield strength of the BADCy/PSU mixtures precured at different temperatures. (c) Flexural yield strain of the BADCy/PSU mixtures precured at different temperatures.

final morphology of the blends was controlled by changing the curing conditions and PSU content.

The PSU phase separated in all the compositions studied, and did not affect the polycyclotrimerization kinetics. The mixtures seemed to have a LCST behavior.

At PSU contents lower than 15 wt %, the mixtures showed spherical domains of PSU dispersed in the BADCy matrix. Phase inversion occurred at around 15 wt % of PSU. At that composition a secondary phase separation was observed and the generated morphologies were highly influenced by the precure temperature. At higher thermoplastic loadings, there was a complete phase inversion. The size of the BADCy nodules slightly increased with the precure temperature.

The SEM and DMA techniques gave the same results. The DMA was also used to calculate the  $T_g$  and composition of the phases. There was an increase of the second component dissolved in each phase with the precure temperature.

The toughness of the PSU-modified matrices increased in all the composition range studied. This improvement was higher as the degree of phase inversion increased.

The mechanical properties such as flexural modulus and strength of the cyanate matrix were not affected by the addition of PSU.

We are grateful for the financial support under contract number MAT95-0701 from Dirección General de Ciencia y Tecnología (DGICYT) (Spain). One of us, I. Harismendy, is indebted to the Ministerio de Educación y Cultura (Spain) for a fellowship grant. Thanks are also extended to Ciba Spec. Chem. Inc. for supplying the cyanate resin used in this work.

## REFERENCES

1. Shimp, D. A. *SAMPE Q* 1987, 19, 41.
2. Mc Connell, V. P. *Adv Compos* 1992, May/June, 28.
3. Hamerton, I. In *Chemistry and Technology of Cyanate Ester Resins*; Hamerton, I., Ed.; Blackie: London, 1994.
4. Cao, Z.; Mechin, F.; Pascault, J. P. *Polym Int* 1994, 34, 41.
5. Harismendy, J.; Del Río, M.; Eceiza, A.; Gavalda, J.; Gómez, C. M.; Mondragon, I. *J Appl Polym Sci*, to appear.
6. Srinivasan, S. A.; McGrath, J. E. *Polymer* 1998, 39, 2415.
7. Kim, Y. S.; Kim, S. C. *Macromolecules* 1999, 32, 2334.
8. Inoue, T. *Prog Polym Sci* 1995, 20, 119.

9. Hourston, D. J.; Lane, J. M. *Polymer* 1992, 33, 1379.
10. Kinloch, A. J.; Yuen, M. L.; Jenkins, S. D. *J Mater Sci* 1994, 29, 3781.
11. Woo, E. W.; Bravened, L. D.; Seferis, J. C. *Polym Eng Sci* 1994, 34, 1664.
12. Hedrik, J. L.; Yilgor, I.; Wilkes, G. L.; McGrath, J. E. *Polym Bull* 1985, 13, 201.
13. Hwang, J. W.; Cho, K.; Park, C. E. *J Appl Polym Sci* 1999, 74, 33.
14. Harismendy, I.; Gómez, C.; Ormaetxea, M.; Martin, M. D.; Eceiza, A.; Mondragon, I. *J Polym Mater* 1997, 14, 317.
15. Halley, P. J.; Mackay, M. E.; George, G. A. *High Perform Polym* 1994, 6, 405.
16. Chen, Y. T.; Macosko, C. W. *J Appl Polym Sci* 1996, 62, 567.
17. Deng, Y.; Martin, G. C. *Polymer* 1996, 37, 3675.
18. Srinivasan, S. A.; McGrath, J. E. *SAMPE Q* 1993, 24, 25.
19. de Graaf, L. A.; Hempenius, M. A.; Moller, M. *Polym Prepr ACS Div Polym Chem* 1995, 36, 787.
20. Yoon, T.; Kim, B. S.; Lee, D. S. *J Appl Polym Sci* 1997, 66, 2233.
21. Riccardi, C. C.; Borrajo, J.; Williams, R. J. J.; Girard-Reydet, R.; Sautereau, H.; Pascault, J. P. *J Polym Sci Part B Polym Phys Ed* 1996, 34, 349.
22. Mondragon, I.; Quintard, I.; Bucknall, C. B. *Plast Rubber Comp Proc Appl* 1995, 23, 351.
23. Fang, D. P.; Riccardi, C. C.; Williams, R. J. J. *Polymer* 1993, 34, 3961.
24. Kinloch, J. A.; Hunston, D. L. *J Mater Sci Lett* 1986, 5, 1207.
25. Hwang, J. W.; Park, S. D.; Cho, K.; Kim, J. K.; Park, C. E.; Oth, T. S. *Polymer* 1997, 38, 1835.
26. Williams, R. J. J.; Rozenberg, B. A.; Pascault, J. P. *Adv Polym Sci* 1997, 128, 95.
27. Bussi, P.; Isida, H. *J Appl Polym Sci* 1994, 53, 441.
28. Woo, E. M.; Shimp, D. A.; Seferis, J. C. *Polymer* 1994, 35, 1658.
29. Cho, J. B.; Hwang, J. W.; Cho, K.; An, J. H.; Park, C. E. *Polymer* 1993, 34, 4833.
30. Shimp, D. A.; Hudock, F. A.; Bobo, W. S. 18th *SAMPE Int Tech Conf* 1986, 851.